

# Scanning Electrochemical Microscopy of Model Neurons: Imaging and Real-Time Detection of Morphological Changes

Johanna M. Liebetrau,<sup>†</sup> Heather M. Miller,<sup>‡</sup> and John E. Baur\*

Department of Chemistry, Illinois State University, Normal, Illinois 61790-4160

Sara A. Takacs, Vipavee Anupunpisit,<sup>§</sup> and Paul A. Garriss

Department of Biological Sciences, Illinois State University, Normal, Illinois 61790-4120

David O. Wipf

Department of Chemistry, Mississippi State University, Mississippi State, Mississippi, 39762

**Living PC12 cells, a model cell type for studying neuronal function, were imaged using the negative feedback mode of a scanning electrochemical microscope (SECM). Six biocompatible redox mediators were successfully identified from a large pool of candidates and were then used for imaging PC12 cells before and after exposure to nerve growth factor (NGF). When exposed to NGF, cells differentiate into a neuron phenotype by growing narrow neurites (1–2  $\mu\text{m}$  wide) that can extend  $>100 \mu\text{m}$  from the cell proper. We demonstrate that carbon fiber electrodes with reduced tip diameters can be used for imaging both the cell proper and these neurites. Regions of decreased current, possibly resulting from raised features not identifiable by light microscopy, are clearly evident in the SECM images. Changes in the morphology of undifferentiated PC12 cells could be detected in real time with the SECM. After exposure to hypotonic and hypertonic solutions, reversible changes in cell height of  $<2 \mu\text{m}$  were measured.**

The scanning electrochemical microscope (SECM) was first used to image biological samples shortly after its introduction in the late 1980s. In its first biological application, the SECM was used to obtain topographic images of grass and *Ligustrum sinensis* leaves and to measure the production of oxygen from an *Elodea* leaf during photosynthesis.<sup>1</sup> More recently, the SECM has become an important tool for investigating phenomena occurring in other living biological systems. For example, Matsue has investigated changes in extracellular oxygen during photosynthesis and

respiration.<sup>2</sup> In a recent series of articles, Mirkin used the SECM to measure redox activity, acid–base reactivities, and topography of different cell types.<sup>3–5</sup>

Our laboratories are interested in investigating the role of neurotransmitter release accompanying morphological changes during neuronal development and degeneration. As such, our goal is to combine the powerful techniques of voltammetry and amperometry that have been used for years in studying neurotransmitter dynamics<sup>6–9</sup> with the imaging and spatial-resolution capabilities of the SECM. This combination of SECM in neurobiological systems with the well-established electrochemical techniques for detection of neurotransmitters at carbon fiber electrodes (CFEs) will make for a powerful tool for the investigation of neurotransmitter dynamics, synaptogenesis, and neurodegeneration in culture.

PC12 cells are a dopamine-releasing immortal cell line established from rat adrenal glands and are commonly used as a model neuronal cell type. They express components for dopaminergic neurotransmission, in particular, releasable dopamine stores, and can differentiate into a number of different cell types. Specifically, we are interested in the differentiation of PC12 cells into a neuron phenotype when exposed to nerve growth factor (NGF).<sup>10–13</sup>

\* Corresponding author. Fax: (309) 438-5538. E-mail: jebaur@ilstu.edu.  
<sup>†</sup> Current address: Eli Lilly and Company, Lilly Corporate Center, Indianapolis, IN 46285.  
<sup>‡</sup> Current address: Department of Chemistry and Biochemistry, Northern Illinois University, DeKalb, IL 60115-2862.  
<sup>§</sup> Visiting researcher from Anatomy Department, Faculty of Medicine, Srinakharinwirot University, Bangkok, Thailand.  
(1) Lee, C.; Kwak, J.; Bard, A. J. *Proc. Natl. Acad. Sci. U.S.A.* **1990**, *87*, 1740–1743.

(2) Yasukawa, T.; Kondo, Y.; Matsue, T. *Chem. Lett.* **1998**, 767.  
(3) Cai, C. X.; Liu, B.; Mirkin, M. V.; Frank, H. A.; Rusling, J. F. *Anal. Chem.* **2002**, *74*, 114–119.  
(4) Liu, B.; Rotenberg, S. A.; Mirkin, M. V. *Proc. Nat. Acad. Sci. U.S.A.* **2000**, *97*, 9855–9860.  
(5) Liu, B.; Cheng, W.; Rotenberg, S. A.; Mirkin, M. V. *J. Electroanal. Chem.* **2001**, *500*, 590–597.  
(6) Travis, E. R.; Wightman, R. M. *Annu. Rev. Biophys. Biomol. Struct.* **1998**, *27*, 77–103.  
(7) Michael, D. J.; Wightman, R. M. *J. Pharm. Biomed. Anal.* **1999**, *19*, 33–46.  
(8) Chen, G. Y.; Ewing, A. G. *Crit. Rev. Neurobiol.* **1997**, *11*, 59–90.  
(9) Clark, R. A.; Ewing, A. G. *Mol. Neurobiol.* **1997**, *15*, 1–16.  
(10) Fujita, K.; Lazarovici, P.; Guroff, G. *Environ. Health Perspect.* **1989**, *80*.  
(11) Levi-Montalcini, R. *Science* **1987**, *237*, 1154–1162.  
(12) Green, L. A.; Tischler, A. S. *Proc. Natl. Acad. Sci. U.S.A.* **1976**, *73*, 2424–2428.  
(13) Batistatou, A.; Greene, L. A. *J. Cell Biol.* **1991**, *115*, 461–471.

Under these conditions, cells send out processes called neurites that can synapse onto other cells. One important goal of our collaborative effort is to investigate the dynamics of neurotransmitter release during the growth of these processes and the formation of synaptic contacts with target cells. The aims of this article are to describe the selection of suitable redox mediators, to compare SECM images of differentiated PC12 cells using several types of electrodes, and to demonstrate that rapid morphological changes of only a few micrometers or less can be detected in real time with the SECM.

## EXPERIMENTAL SECTION

**Solutions.** All mediators were prepared at a concentration of 1.0 mM in Hank's balanced salt solution (HBSS, Sigma, St. Louis, MO) with 10 mM HEPES (Sigma) and adjusted to pH 7.4 with 1 M NaOH. The mediators were reagent grade and were used as received from commercial sources. For the experiments involving changes in the buffer osmotic strength, a 50-mL aqueous stock solution was prepared consisting of 10 mM  $\text{Ru}(\text{NH}_3)_6\text{Cl}_3$ , 50 mM D-(+)-glucose, 100 mM HEPES, 50 mM KCl, and 12 mM  $\text{MgCl}_2 \cdot 6\text{H}_2\text{O}$ . Solutions of variable ionic strength were then prepared by pipetting 5.00-mL aliquots of the stock solution into 50-mL volumetric flasks containing variable amounts of NaCl. The concentrations of NaCl in the test solutions were 522, 265, and 0 mM. Aqueous solutions were prepared in 18  $\text{M}\Omega \cdot \text{cm}$  deionized water (NanoPure system, Barnstead-Thermolyne, Inc., Dubuque, IA).

The solution used for polymer-insulating reduced-size electrodes was prepared by dissolving 90 mM 2-allylphenol (98% purity, Aldrich) in a solution of 2 wt % 2-butoxyethanol (99% purity, Aldrich) in 25.0 mL of a 1:1 methanol/water mixture.<sup>14</sup> After adjusting the pH to 9.0 with 10 M  $\text{NH}_4\text{OH}$ , this solution was added to 160  $\mu\text{L}$  of liquefied phenol (90% w/w, Fisher Scientific) for a total volume of 25 mL. The total concentration of phenol was 60 mM.

Microspherical substrates that served as inert models for the cells were prepared by sprinkling Polybead 10- $\mu\text{m}$  polystyrene microspheres (Polysciences, Inc., Warrington, PA) on the surface of a tissue culture plate coated with a fine film of epoxy.

**Electrodes.** All of the electrodes used for SECM experiments were prepared from carbon fibers with nominal radii of 5  $\mu\text{m}$  (Thornel P-55, Cytac, Greenville, SC). Carbon fiber electrodes (CFEs) sealed in glass were prepared as described previously.<sup>15</sup> The electrode tip was polished at 90° on a micropipet beveller (model BV-10, Sutter Instrument, Novato, CA) and rinsed in warm toluene. For experiments involving ascorbic acid and  $\text{IrCl}_6^{3-}$ , the electrode was pretreated by applying a 3.0-V triangle wave to the electrode, then a constant potential of 1.5 V, each for a period of 7 s in a solution of 1 M NaOH.<sup>16</sup>

Polymer-insulated carbon fiber electrodes were constructed in a manner similar to that developed by Strein and Ewing.<sup>14</sup> A carbon fiber was inserted into a pulled glass capillary so that ~1 cm of fiber protruded from the tapered end of the capillary. Epoxy

was next drawn into the tip of the electrode via capillary action, and the carbon fiber was immediately dipped briefly into acetone to remove epoxy from the surface of the exposed carbon fiber. After curing at 150 °C for 2 h, the fiber was insulated by applying a potential of 4.0 V vs a platinum wire counter/reference electrode for 25 min in a solution of 90 mM 2-allylphenol and 60 mM phenol. Electrodeposition times <25 min resulted in incomplete insulation. After curing the polymer at 150 °C for 30 min, a cyclic voltammogram was recorded; complete insulation was indicated by the absence of faradaic current. Finally, the tip of the insulated carbon fiber was trimmed with a scalpel to a length of approximately 1 mm, and the tip was polished at 90° to obtain a flat disk surface.

Polymer-insulated flame-etched carbon fiber electrodes were prepared as described for the polymer-insulated CFEs, except that the tip of the protruding carbon fiber was passed quickly through the flame of a Bunsen burner just before the polymer insulation step. Immediately prior to use, all electrodes were polished at a 90° angle on a micropipet beveller.

**Instrumentation.** All cyclic voltammetry was performed using a BAS 100-W voltammetric analyzer (Bioanalytical Systems, West Lafayette, IN). An EI-400 bipotentiostat (Cypress Systems, Inc., Lawrence, KS) with an external function generator (Krohn-Hite Corporation, model 1400A, Avon, MA) was used for electropolymerization and electrode pretreatment.

The SECM was similar to that described previously,<sup>17</sup> except that it was adapted to fit the stage of an inverted microscope (Olympus America, Melville, NY) equipped with a digital camera (Sony Corporation of America, New York, NY). The electrochemical cell, consisting of the carbon fiber microelectrode, a platinum wire auxiliary electrode, and a 3 M Ag/AgCl reference electrode, was positioned in a transparent polystyrene tissue culture dish containing the substrate and mediator solution. The culture plate was mounted to the stage of the microscope, and an EI-400 bipotentiostat was used to control the tip potential and measure the tip current. Positioning and data acquisition were controlled with a PC via an interface module and SECM software. Approach curves were recorded at a scan rate of 2  $\mu\text{m/s}$ ; linescans and images were recorded at a scan rate of 10  $\mu\text{m/s}$ .

For the experiments requiring a change in osmotic strength, the tip was lowered until the current was 75% of  $i_{T,\infty}$  (~3  $\mu\text{m}$  above the PC12 cell surface) and held stationary. Solutions of variable ionic strength were discharged by pressure ejection near the cell using a micropipet attached to a Picospritzer II (General Valve Corp., Fairfield, NJ). The size of the opening at the tapered end of the micropipet was ~10  $\mu\text{m}$ . The filled micropipet was lowered to the cell surface with the aid of a manual micropositioner (Narishige, Tokyo) and the SECM video system.

Dopamine release was determined by HPLC-EC (BAS 200B with a Unijet detector and injector, Bioanalytical Systems, West Lafayette, IN) using a millibore, reverse-phase column (Phase-II, ODS 3  $\mu\text{m}$ , 100  $\times$  3.2 mm, Bioanalytical Systems). The electrochemical detector was set at a potential of +550 mV. The mobile phase was pumped at a rate of 1 mL/min and consisted of (per 2 L of water) 0.5 g EDTA, 0.4 g octane sulfonic acid, 24.56 g of monochloroacetic acid, 1.16 g of sodium chloride, and 50 mL of

(14) Strein, T. G.; Ewing, A. G. *Anal. Chem.* **1992**, *64*, 1368–1373.

(15) Kelly, R. S.; Wightman, R. M. *Anal. Chim. Acta* **1986**, *187*, 79–87.

(16) Anjo, D. M.; Kahr, M.; Khodabakhsh, M. M.; Nowinski, S.; Wanger, M. *Anal. Chem.* **1989**, *61*, 2603–2608.

(17) Wipf, D. O.; Ge, F.; Spaine, T. W.; Baur, J. E. *Anal. Chem.* **2000**, *72*, 4921–4927.

Table 1. Results of the Biocompatibility Testing for Selected Mediators<sup>a</sup>

mediator (1mM)	% viability	cell appearance	DA release (ng/2 h)
Hank's buffer (control)	90.0	ok	0.280
<b>IrCl<sub>6</sub><sup>3-</sup></b>	92.6	ok	0.151
<b>Ru(NH<sub>3</sub>)<sub>6</sub><sup>3+</sup></b>	89.8	unhealthy, change in morphology, cell membrane budding after 2 h of exposure	0.331
<b>L-ascorbic acid</b>	89.7	ok	0.442
4-methylcatechol	72.5	cell membrane budding, broken and swollen cells	0.716
<b>1,4-benzoquinone</b>	89.0	some cells are ok, some have patterns as in 4-methylcatechol	0.507
<b>4-hydroxyTEMPO</b>	88.5	unhealthy, cell membrane budding	— <sup>b</sup>
TEMPO	94.2	unhealthy	—
2,5-dihydroxy-1,4-benzo-quinone	56.4	change in morphology	0.223
1,4-naphtho-quinone	0	cell lysis	—
1,2-naphthoquinone	0	cell lysis	—
Safranin T	39	staining inside cell	—
methylene blue	73.2	staining inside cell	—
5-hydroxy-1,4-naphthoquinone	0	cell lysis	—

<sup>a</sup> Cultured PC12 cells were exposed to 1 mM concentrations of each redox mediator for 2 h prior to the trypan blue exclusion assay or HPLC-EC. Mediators in boldface type were selected for further evaluation as mediators for SECM imaging. <sup>b</sup> HPLC-EC was not performed on cells in that mediator.

acetonitrile. The pH of the mobile phase was adjusted to 2.8 using sodium hydroxide.

**PC12 Cells.** PC12 cells were obtained from American Type Culture Collection (Manassas, VA) and were cultured in collagen-coated culture flasks (25 cm<sup>2</sup>, Nalge Nunc International). Cells were maintained in RPMI-1640 medium (Sigma) supplemented with 10% horse serum 5%, fetal bovine serum (Atlanta Biological), and penicillin–streptomycin antibiotics (Sigma) and were incubated at 37 °C in a humidified atmosphere of 95% air and 5% carbon dioxide. Twenty-four hours prior to conducting SECM experiments, cells were plated on collagen-coated polystyrene tissue culture dishes (60 × 15 mm, Corning) and incubated. Upon removal from the incubator, the growth medium was replaced with mediator solution, and SECM experiments were then conducted under ambient laboratory conditions. Cells were selected for imaging on the basis of gross morphology; those that were slightly elongated in appearance exhibited the greatest tendency to remain adhered to the collagen surface during the imaging process. Cell clusters and those cells that appeared to be not well-adhered to the collagen were avoided. All SECM experiments were completed within 90 min of removing culture plates from the incubator.

For dopamine release experiments, PC12 cells (2.5 × 10<sup>4</sup> cells/well) were plated in a collagen-coated (7 μg/cm<sup>2</sup>) 96-well plate (Becton Dickinson) and allowed to adhere for 1–2 days in supplemented RPMI 1620 medium (Sigma). At the time of experimentation, culture medium was removed while simultaneously adding release medium (HBSS, Sigma) using a cassette peristalsis pump (Monostat Corporation). A 200-μL portion of medium was then drawn out of each well, leaving ~150 μL. Release medium contained 10 mM HEPES (Sigma) and 1.0 mM ascorbic acid (Sigma) at a pH of 7.4. After 120 min of incubation, 100 μL medium was removed, taking care not to aspirate any cells; placed in a microcentrifuge tube; and treated with 5 μL of 2 N perchloric acid to preserve dopamine. Samples were frozen at –80 °C for at most 2 days before assay. For conditions of the release experiments, dopamine release from PC12 cells was calcium-dependent and enhanced by potassium depolarization (data not shown).

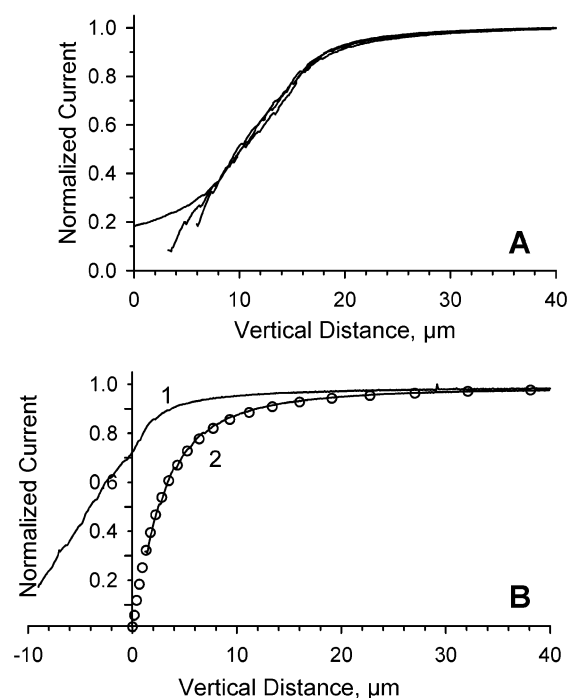


Figure 1. (A) Approach of a glass-insulated 10-μm-diameter CFE to three different PC12 cells using 1.0 mM Ru(NH<sub>3</sub>)<sub>6</sub><sup>3+</sup> as the mediator. (B) Approach of the same electrode to a 10-μm-diameter polystyrene bead (curve 1) and the planar support (curve 2). Open circles represent the calculated approach curve to a planar substrate for a 10-μm-diameter electrode with RG = 2.03. The zero vertical distance for curve 1 is the estimated point at which the electrode made contact with the top of the bead.

Cell viability was measured using the trypan blue exclusion method. Adherent cells were removed by titration. A 100-μL portion of the cell suspension was collected and diluted 1:10 by adding 800 μL of sterile medium and 100 μL of trypan blue (0.4%, Sigma). After 5 min following addition of the dye, ~15 μL of solution was transferred to a hemocytometer for counting.

## RESULTS AND DISCUSSION

**Mediator Selection.** Redox mediators used for feedback imaging must meet several criteria. First, the mediator must be

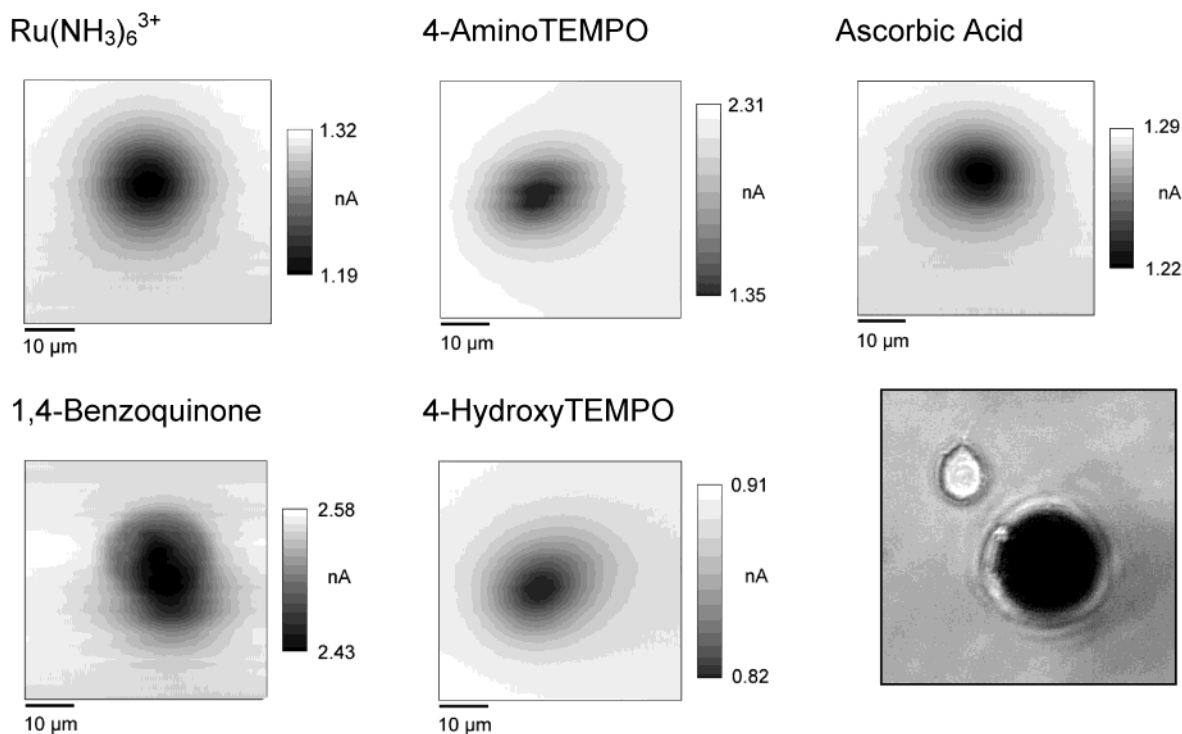


Figure 2. SECM feedback images of individual PC12 cells recorded with a glass-insulated 10- $\mu\text{m}$ -diameter CFE in different mediators (1.0 mM each). An optical micrograph (lower right) illustrates the overall size of the electrode ( $\sim 25\text{-}\mu\text{m}$  diameter) relative to a typical cell.

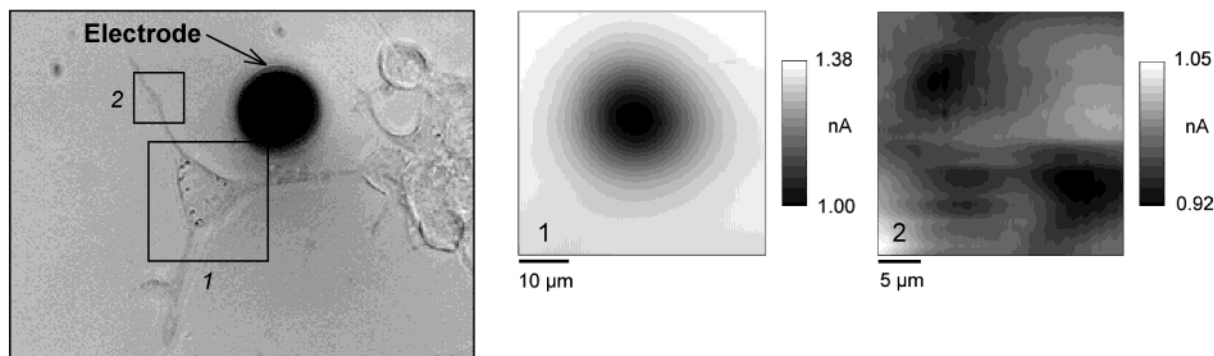


Figure 3. Optical and SECM images of differentiated PC12 cells. The SECM images were recorded at the boxed areas indicated in the optical micrograph using a glass-insulated 10- $\mu\text{m}$ -diameter CFE in 1.0 mM  $\text{Ru}(\text{NH}_3)_6^{3+}$ .

nontoxic to cells, at least over the time course of the experiment. Second, the release of electroactive species by the cell must not be adversely affected by the presence of the mediator. Third, the redox potential of the mediator should be distinct from the redox potential of these released species. Although previous studies have used mediators with redox potentials negative enough to require deoxygenation of the medium,<sup>3–5</sup> we elected to avoid these mediators, because hypoxia affects cell function. Finally, the mediators must exhibit good electrochemistry at CFEs, because these are the electrodes of choice for detection of aminergic neurotransmitter release.<sup>18</sup>

An extensive list of redox mediators was compiled from the literature,<sup>19,20</sup> and the list was condensed to the mediators shown in Table 1. Although this list contains both membrane-permeable

and membrane-impermeable mediators, relatively high concentrations were used so that imaging was solely based upon negative feedback, and contributions of intracellular redox reactions of the mediator would not be evident.<sup>5</sup> For each mediator, cell viability was evaluated with the trypan blue exclusion test and by a visual inspection of the cells during exposure to a 1 mM solution of the mediator. Additionally, the effect of the mediator on dopamine release was evaluated at the whole-plate level with HPLC.<sup>21</sup> The results of these tests are also shown in Table 1.

On the basis of the results of this biocompatibility testing, five mediators were selected for imaging experiments. The selected mediators are shown in boldface type in Table 1. Populations of cells exposed to each of these mediators exhibited viabilities near 90% (note that for the control, Hank's buffer, cells also exhibited 90% viability), and similar dopamine release, although some changes in cell appearance were observed. For example, after

(18) Baur, J. E.; Kristensen, E. W.; May, L. J.; Wiedemann, D. J.; Wightman, R. M. *Anal. Chem.* **1988**, *60*, 1268–72.

(19) Fultz, M. L.; Durst, R. A. *Anal. Chim. Acta* **1982**, *140*, 1–18.

(20) Johnson, J. M.; Halsall, H. B.; Heineman, W. R. *Anal. Biochem.* **1983**, *133*, 186–189.

(21) Garris, P. A.; Walker, Q. D.; Wightman, R. M. *Brain Res.* **1997**, *753*, 225–234.



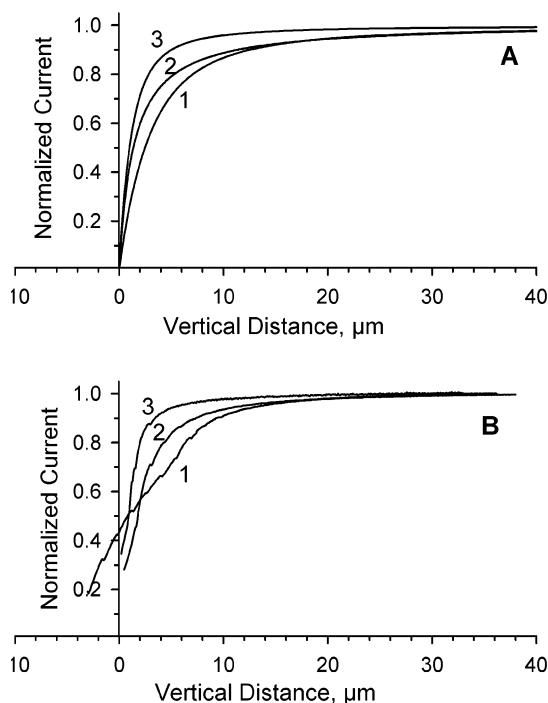


Figure 4. Comparison of theoretical and experimental approach curves at three different types of CFEs: (A) calculated approach curves for  $RG = 2.03$  and  $r = 5 \mu\text{m}$  (curve 1),  $RG = 1.11$  and  $r = 5 \mu\text{m}$  (curve 2), and  $RG = 2.03$  and  $r = 2 \mu\text{m}$  (curve 3), corresponding to a glass-insulated  $10\text{-}\mu\text{m}$ -diameter CFE, a polymer-insulated  $10\text{-}\mu\text{m}$ -diameter CFE, and a polymer-insulated flame-etched CFE, respectively; and (B) experimental curves for approach to individual PC12 cells using the corresponding electrodes in  $1.0 \text{ mM Ru}(\text{NH}_3)_6^{3+}$ .

exposure to  $\text{Ru}(\text{NH}_3)_6^{3+}$  for more than 2 h, cells began to appear unhealthy and exhibit changes in morphology. To avoid viability concerns when using  $\text{Ru}(\text{NH}_3)_6^{3+}$ , therefore, experiments were terminated after 90 min of exposure of the cells to this mediator. Upon exposure to 1,4-benzoquinone, a membrane-permeable mediator, the appearance of some cells was unchanged, but others exhibited gross morphological changes. Therefore, in experiments using 1,4-benzoquinone as the mediator, only the cells with a healthy appearance were selected. Although these results showed that exposure to the stable nitroxide free radical 4-hydroxyTEMPO resulted in an unhealthy cell appearance, additional studies have shown that this compound and the related 4-aminoTEMPO do not adversely affect the viability of the cells.<sup>22</sup> Consequently, the nitroxide mediators were also selected for additional experiments. Although it exhibits good biocompatibility,  $\text{IrCl}_6^{3-}$  was not selected for further use because it exhibited poor electron transfer kinetics at both untreated and electrochemically treated CFEs.

**SECM of PC12 Cells.** Figure 1A shows typical approach curves recorded at a  $10\text{-}\mu\text{m}$  diameter CFE for three different PC12 cells. Because of the difficulty in determining the contact point between the electrode and the cell, the zero point for these data could not be determined, and therefore, the distance axis is relative. Using the membrane-impermeable mediator  $\text{Ru}(\text{NH}_3)_6^{3+}$ , purely negative-feedback approach curves are expected. Although the current decreases as the cell is approached, it does not drop sharply toward zero as expected. Rather, below a normalized

current of  $\sim 0.8$ , the slope becomes shallower and nearly plateaus in one case.

To investigate this deviation from expected behavior further, a model substrate was prepared by floating  $10\text{-}\mu\text{m}$  diameter polystyrene beads on a thin layer of a viscous epoxy on the bottom of a cell culture dish. After the epoxy was cured, the spherical beads extended  $8\text{--}10 \mu\text{m}$  above the planar epoxy layer, resulting in a substrate similar in size and relief to the PC12 cells. Figure 1B shows approach curves recorded with a  $10\text{-}\mu\text{m}$ -diameter CFE to a single polystyrene bead (curve 1) and the planar epoxy support (curve 2). The theoretical response of an electrode approaching a planar substrate is represented by the open circles.<sup>23,24</sup> The agreement between theory and experiment in the planar case is very good, whereas the approach curve recorded at the polystyrene bead deviates from theory and more closely resembles those recorded at the PC12 cells. The normalized current initially decreases to  $0.7\text{--}0.8$ , after which the curve broadens and only slowly approaches 0. Observation of the electrode tip during the approach reveals that the electrode makes contact with the top of the bead when the normalized current is  $0.7\text{--}0.8$ . Because the bead and the fiber are the same diameter and when the two make contact, mediator can still reach the electrode surface. As the electrode was lowered further, two things were observed: the bead deformed and the electrode tip bent. As this occurred, the available electroactive surface decreased, albeit more slowly than for approach to a planar substrate, resulting in anomalous approach curves. Because cells are less rigid than the polystyrene bead, the shape of the approach curves for the cells (Figure 1A) are likely to be dominated by deformation of the cell rather than bending of the electrode. Differences in cell curvature, rigidity, and movement under the pressure of the electrode will result in variations in the approach curves recorded at different cells. Since it was difficult to define the exact point when the electrode and cell touched and to avoid injuring the cell, imaging was conducted only when the normalized current was greater than 0.85.

SECM images of different PC12 cells recorded in five mediators are shown in Figure 2. Also shown is a micrograph of a glass-insulated  $10\text{-}\mu\text{m}$  CFE next to a typical cell. Note that the electrode appears much larger than the cell because the  $10\text{-}\mu\text{m}$  diameter fiber is encapsulated in a glass insulating sheath, and the two are indistinguishable under the lighting conditions. To record the SECM images, the electrode was placed over the apex of the cell, and the electrode was lowered to 85% of the current measured far from the substrate,  $i_{T,\infty}$ . Although the general cell shape is discernible in these images, little detail is produced by the relatively large probe.

**Differentiated PC12 Cells.** After exposure to nerve growth factor (NGF), PC12 cells grow neurites that extend out from the cell proper and can make connections to other cells. An example of such a differentiated cell is shown in the micrograph of Figure 3. This micrograph also shows a CFE for size comparison. When differentiated, the cell proper flattens and becomes irregularly shaped. The neurites are thin ( $1\text{--}3 \mu\text{m}$  in diameter) and do not extend as far above the collagen support as the cell proper. These characteristics produce challenges for imaging differentiated cells. Because the electrode is rastered at a constant height above the

(22) Takacs, S. A.; Garriss, P. A. Unpublished results.

(23) Amplett, J. L.; Denuault, G. *J. Phys. Chem. B* **1998**, *102*, 9946–9951.

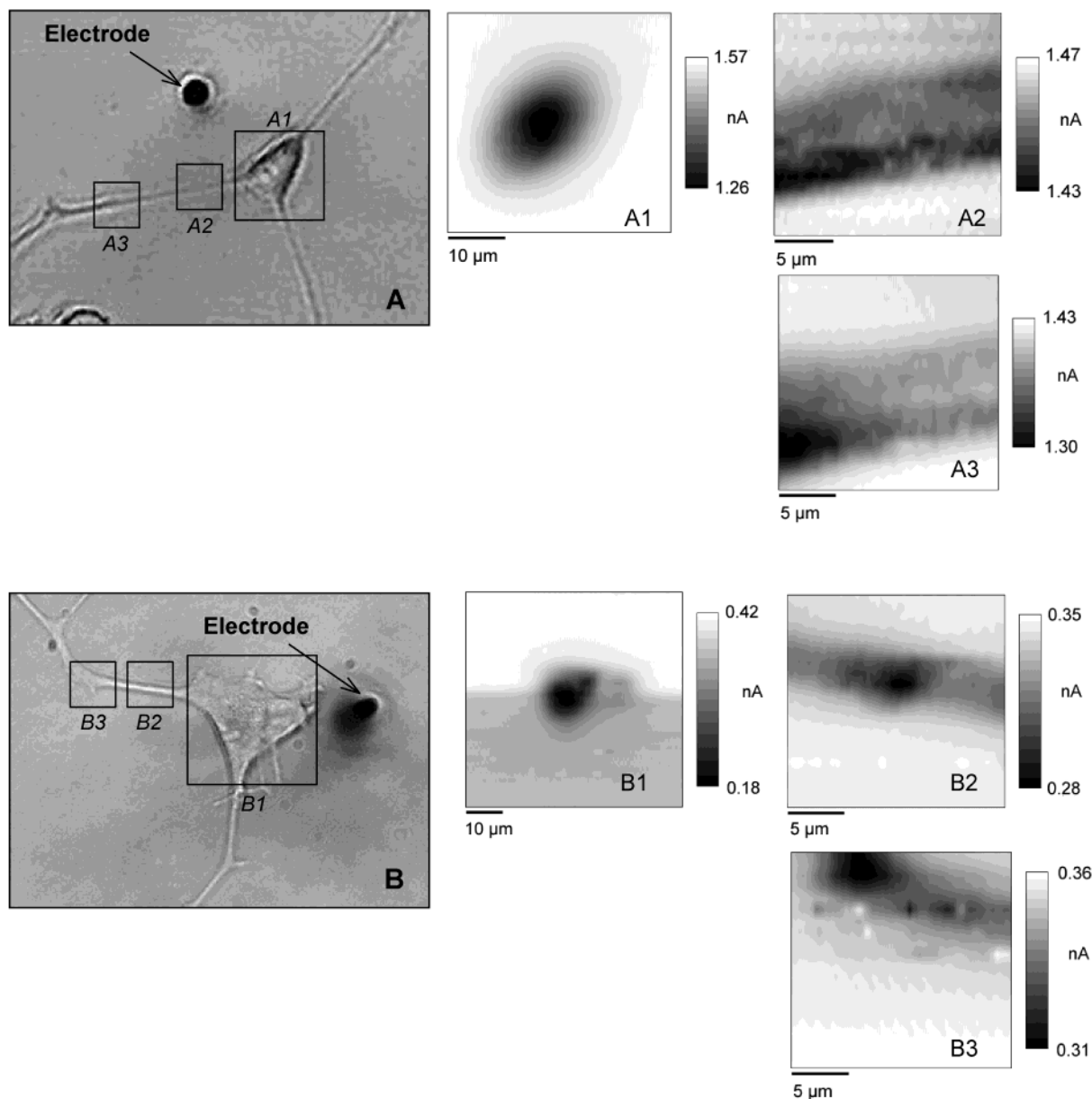


Figure 5. Optical and SECM images of differentiated PC12 cells recorded using (A) a polymer-insulated 10- $\mu\text{m}$ -diameter CFE and (B) a polymer-insulated flame-etched CFE. The SECM images were recorded at the areas indicated in the micrographs using 1.0 mM  $\text{Ru}(\text{NH}_3)_6^{3+}$  as the mediator.

substrate, the neurites are too low to be imaged when the electrode is placed at the apex of the cell proper. Additionally, the cell proper often exhibits raised areas (perhaps corresponding to intracellular organelles) after differentiation, even making the imaging of the entire cell proper impossible. For these reasons, the entire differentiated cell cannot be imaged at once. Instead, regions of interest must be imaged separately, with the electrode placed at the optimal vertical position for each region.

It is evident from the micrograph of Figure 3 that the CFE is significantly larger than the structures it is being used to image. As a result, the SECM image of the cell proper is indistinct, and the triangular shape is not evident. Imaging of the low-lying neurite proved to be even more problematic. With such a large tip (relative to the substrate features), it proved difficult (often impossible) to lower the probe close enough so that it did not collide either with the neurite or with the collagen support. A typical SECM image

of a neurite is also shown in Figure 3; no distinct image is visible because the relatively large CFE made contact with the neurite during the raster, stretching it in both directions for several micrometers until it snapped back to its original position. Similar problems were occasionally encountered when imaging undifferentiated PC12 cells with these electrodes. Occasionally, if the probe was not completely flat, it made contact with the cell during the raster, resulting in a slow-motion movement of the cell in the direction of the minor axis of the raster.

For these reasons, smaller CFEs were used for subsequent experiments. These electrodes were prepared by insulating cylindrical carbon fiber electrodes with a phenolic polymer.<sup>14</sup> Two types of polymer-insulated electrodes were used. In the first, a 10- $\mu\text{m}$  carbon fiber was coated with a 1–2- $\mu\text{m}$ -thick layer of polymer, and the tip was exposed by polishing at 90° on a micropipet beveller. The resulting tip had an overall diameter of

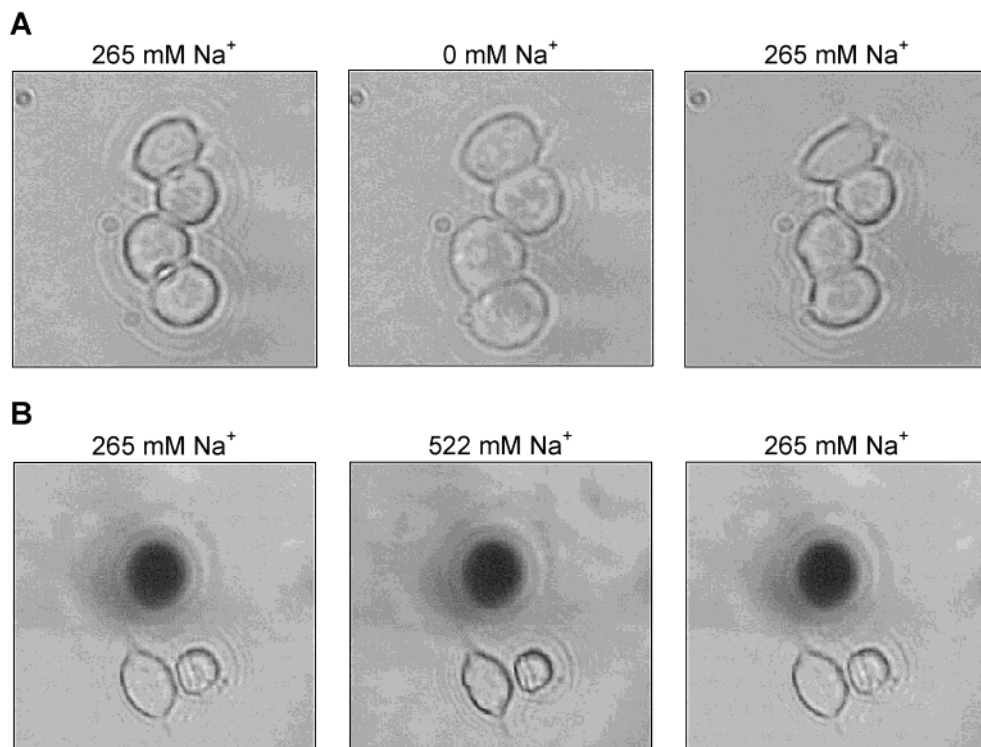


Figure 6. Optical micrographs of PC12 cells exposed to (A) an increase and (B) a decrease in buffer osmotic strength. Cells are shown before, during, and after the change in osmotic strength. A polymer-insulated 10- $\mu\text{m}$  CFE is shown in the lower panels for scale.

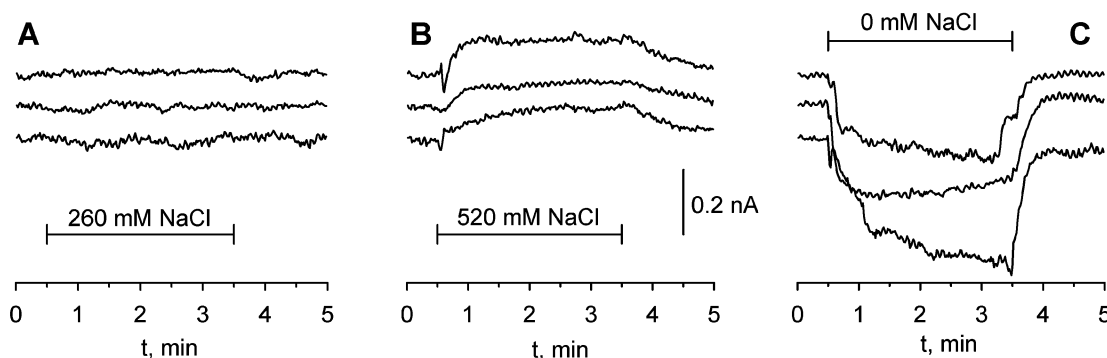


Figure 7. Real-time measurements of the heights of individual PC12 cells during changes in solution osmotic strength recorded with a polymer-insulated 10- $\mu\text{m}$ -diameter CFE. The cells were immersed in a buffer with 260 mM NaCl and a micropipet-ejected buffer with (A) 260 mM NaCl (a control), (B) 0 mM NaCl, or (C) 520 mM NaCl onto the cell. All solutions also contained 1.0 mM  $\text{Ru}(\text{NH}_3)_6^{3+}$  as the mediator. The curves, each recorded at different cells, are offset for clarity.

$\sim 12\text{--}14\ \mu\text{m}$ , as compared to the  $20\text{--}25\ \mu\text{m}$  for the glass-insulated CFEs used above. For the second type of electrode, the carbon fiber was flame-etched prior to insulation. The resulting carbon fiber typically had a diameter of  $2\text{--}3\ \mu\text{m}$ ; when insulated, therefore, the overall tip diameter was approximately  $4\text{--}7\ \mu\text{m}$ .

For a planar substrate, the slope of the negative feedback approach curves should be steeper as the electrode size and insulation thickness (expressed as RG, the ratio of the overall tip radius to the radius of the conductor) are reduced.<sup>23,24</sup> This is demonstrated in Figure 4A, which shows theoretical approach curves to a planar substrate calculated for the three types of electrodes used in this work: a 10- $\mu\text{m}$ -diameter carbon fiber sealed in glass with an overall tip diameter of  $20\ \mu\text{m}$  ( $\text{RG} = 2$ ), a 10- $\mu\text{m}$ -diameter polymer-insulated carbon fiber (overall tip diameter  $12$

$\mu\text{m}$ ,  $\text{RG} = 1.2$ ), and a 2- $\mu\text{m}$ -diameter polymer-insulated etched carbon fiber (overall tip diameter  $4\ \mu\text{m}$ ,  $\text{RG} = 2$ ). Note that these exact values of RG are not available in reference,<sup>23</sup> so the closest values of RG available in that work were used (2.03 and 1.11). This theory predicts that the polymer-insulated electrodes should have steeper approach curves and, therefore, will be more sensitive to the tip-substrate separation.

As shown by the experimental approach curves in Figure 4B, the smaller tips also allow for closer approaches to the nonplanar cells. Whereas the relatively large tip of the glass-insulated CFE makes contact with the cell when the normalized current drops to  $0.7\text{--}0.8$ , the electrodes with smaller tips drop sharply toward 0 until the normalized current is  $0.3\text{--}0.4$ . These results suggest that the smaller electrodes can be used for imaging much closer to the substrate and that they will be much more sensitive to changes in substrate morphology.

(24) Mirkin, M. V.; Fan, F. R. F.; Bard, A. J. *J. Electroanal. Chem.* **1992**, 328, 47–62.

SECM images of differentiated PC12 cells recorded with the smaller electrodes and the corresponding optical micrographs are shown in Figure 5. For size comparison, the electrodes are also shown in the micrograph. For the polymer-insulated 10- $\mu$ m-diameter CFE (Figure 5A), the SECM image of the cell proper closely resembles the slanted, oblong cell proper in the photograph. The SECM also produced distinct images of the neurites, with well-defined regions of decreased current, corresponding to raised features on the neurite. For the etched electrode (Figure 5B), the SECM image of the cell proper does not resemble the micrograph. This particular cell had a raised structure near the center of the cell proper; thus, the electrode had to be positioned above this structure to avoid collisions with it when imaging the cell proper. The remaining cell proper is not visible because of the sharp distance dependence of the current for this electrode. However, this large distance sensitivity is especially advantageous for imaging the neurites, as shown in panels B2 and B3 of Figure 5. The neurites are more well-defined than the cell proper, and very distinct regions of decreased current are evident in the SECM images. We postulate that these regions of decreased current are the result of raised structures that are not visible in the optical micrograph. However, they could also be chemical in origin if the mediator is reduced by some secreted species or if such a secreted species is oxidized at the tip, thus partially offsetting the cathodic mediator current.

These data show that the smaller electrodes are useful for examining detailed morphology of small areas of the differentiated PC12 cells. However, larger regions cannot be imaged simultaneously because of the large relief of the substrate and the short working distance of these smaller electrodes.

**Real-Time Measurement of Changes in Cell Height.** To demonstrate the usefulness of the SECM for measuring small changes of cell morphology in real time, an experiment was designed to induce reversible changes in cell size by changing the ionic strength of the medium surrounding the cells.<sup>25</sup> To make these measurements, a polymer-insulated 10- $\mu$ m-diameter CFE was placed just above the highest point of an individual PC12 cell. Solutions containing identical concentrations of mediator but differing concentrations of Na<sup>+</sup> were pressure-ejected from a micropipet pointed toward the cell. Cells exposed to hypertonic conditions (increased ionic strength) shrink as a result of a net loss of water from osmosis. As a consequence, the tip–substrate distance increases, resulting in an increase in tip current. Conversely, cells exposed to hypotonic conditions (decreased ionic strength) gain water and swell. The resulting decrease in tip–substrate separation is measured as a lower tip current.

Because changes in solution ionic strength cause a change in the mediator activity, ejection of the differing ionic strength buffers may result in a change in current measured with the probe even in the absence of a change in cell size. To correct for this background change, an additional measurement was made with the CFE withdrawn above the cell surface to a distance where current would not be influenced by changes in the cell morphology. The change in current attributable to a change in cell height was then obtained by subtracting this background current from the current measured with the CFE close to the cell.

Figure 6 shows two sequences of micrographs before, during, and after exposure of the cells to hypotonic or hypertonic conditions. The change in overall size is subtle but is evidenced by the change in sharpness of the cells' edges. The boundaries of larger cells have less contrast than the boundaries of smaller cells. Additionally, the change in size is reversible, as demonstrated by the return of cells to their original size following the change in ionic strength.

The background-corrected responses of several cells to different solutions ejected from the micropipet are shown in Figure 7. Under isotonic conditions (i.e., solution in the micropipet identical to the bulk solution), the current shows no distinct change, indicating that there is no change in tip–substrate separation distance. Under hypertonic conditions (520 mM Na<sup>+</sup>), however, the current rapidly increases after the application of the solution with a lower ionic strength as the cell shrinks. The current returns to the original value, indicating recovery of the cell following the termination of the stimulus, although this recovery is slower than the initial change in size. The change in height for these cells is calculated to be between 0.75 and 1.0  $\mu$ m from the approach curves. Upon exposure to hypotonic conditions (0 mM Na<sup>+</sup>), a large decrease in current is recorded as the cell height increases. After removal of the stimulus, the cell rapidly returns to its original size. The overall increase in the cell size, calculated by comparison to the approach curves, is between 1.5 and 2.0  $\mu$ m.

## CONCLUSIONS

With the ongoing interest in elucidating cell structure–function relationships, there is an increasing need for a technology that allows investigations of living cells as dynamic systems. The SECM is uniquely suited to such investigations because of its potential to record the release of electroactive species concomitantly with morphological change. We have shown that differentiated PC12 cells, model dopamine-releasing neurons, can be imaged with high resolution. Distinct regions of decreased feedback current, possibly arising from variable surface topography not visible with a light microscope, are clearly visible in the SECM images of the neurites extended by these cells. With additional refinement of the probe and imaging methodology, these localized regions will be probed for more spatial detail and electrochemical activity.

The results presented here also demonstrate another remarkable feature of the SECM: its capability to record real-time morphological changes. Induced morphological changes of <1  $\mu$ m were detected by monitoring the current produced by an electrode placed close to the cell. Further reduction in tip size should allow for closer placement of the probe at the cell surface and a greater sensitivity of the probe in response to changes in the cell height. Such improvements should lead to the ability to detect real-time morphological changes not observable with the light microscope.

Constant height imaging is less than optimal for imaging samples with high relief. We have recently added a current-based constant distance feedback mechanism<sup>26</sup> that allows the probe to follow vertical contours of the substrate. With this advancement, topographical measurements of the cell proper and the narrow, low lying neurites of differentiated PC12 cells can be made in a

(25) Borges, R.; Travis, E. R.; Hochstetler, S. E.; Wightman, R. M. *J. Biol. Chem.* **1997**, *272*, 8325–8331.

(26) Wipf, D. O.; Bard, A. J. *Anal. Chem.* **1993**, *65*, 1373–1377.



single frame.<sup>27</sup> Constant distance imaging with shear force<sup>28,29</sup> or impedance<sup>30</sup> feedback would allow simultaneous recording of topography and neurotransmitter release from the cells.

---

(27) Kurulugama, R.; Baur, J. E.; Garris, P. A.; Wipf, D. O. Unpublished results.

(28) Hengstenberg, A.; Kranz, C.; Schuhmann, W. *Chem. Eur. J.* **2000**, *6*, 1547–1554.

(29) Buchler, M.; Kelley, S. C.; Smyrl, W. H. *Electrochem. Solid-State Lett.* **2000**, *3*, 35–38.

(30) Alpuche-Aviles, M. A.; Wipf, D. O. *Anal. Chem.* **2001**, *73*, 4873–4881.

#### ACKNOWLEDGMENT

This work was supported by a grant from the National Science Foundation (DBI-9987028). We are grateful to Rick Crouse, Kim Garris, and Angieska Stadnick for technical assistance.

Received for review September 25, 2002. Accepted November 13, 2002.

AC026166V